ISSN 1615-9306 · JSSCCJ 45 (16) 2022 · Vol. 45 · No. 16 · August 2022

Journal of SEPARATION SCIENCE

16|2022

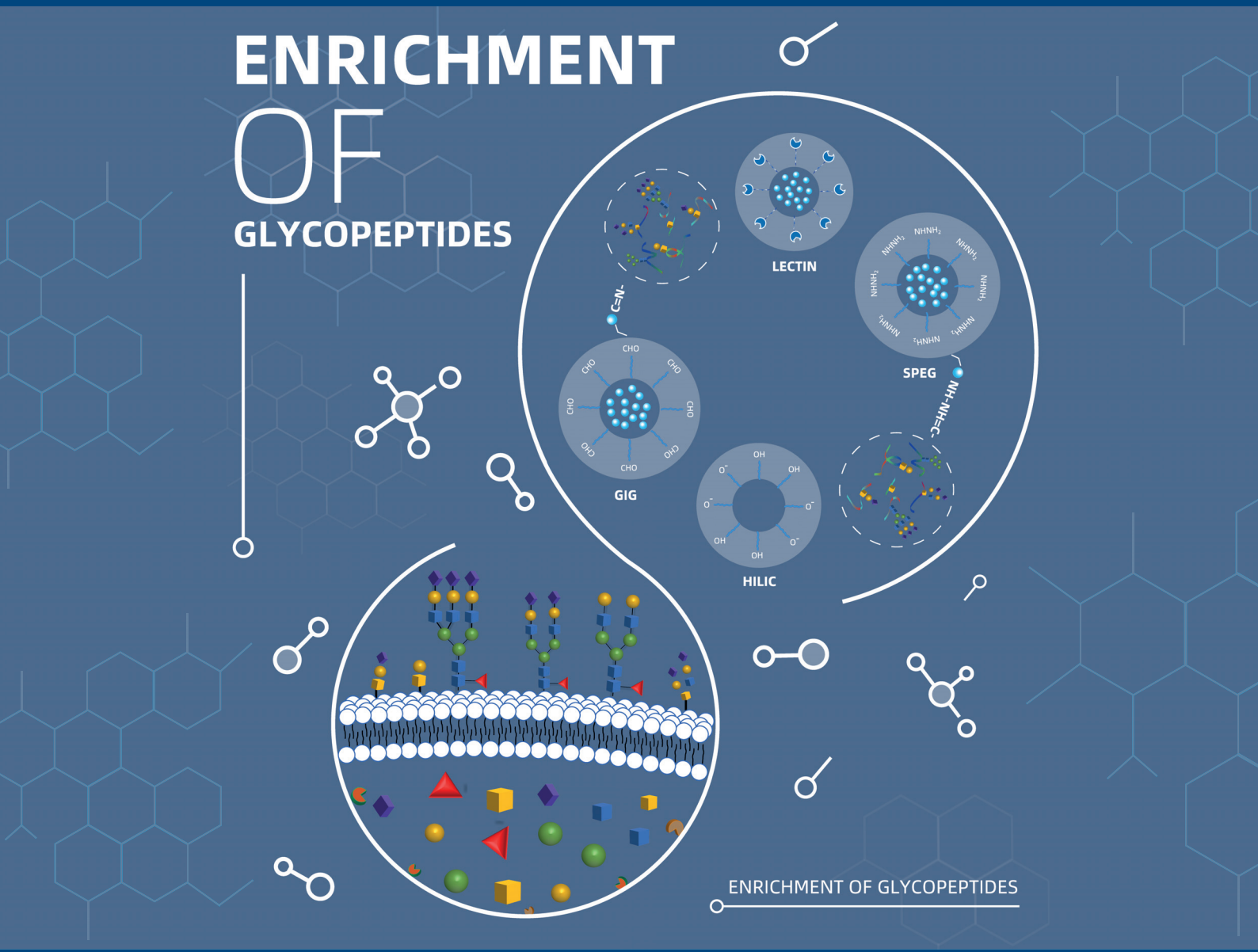

www.jss-journal.com

Methods
Chromatography · Electroseparation

Applications
Biomedicine · Foods · Environment

WILEY-VCH

Received: 17 May 2022 | Revised: 5 July 2022 | Accepted: 5 July 2022

DOI: 10.1002/jssc.202200402

JOURNAL OF SEPARATION SCIENCE

RESEARCH ARTICLE

Liquid chromatography-dielectric barrier discharge ionization mass spectrometry for the analysis of neutral lipids of archaeological interest

Marcos Bouza[1] | **Julio García-Martínez**[1] | **Bienvenida Gilbert-López**[1,2] | **David Moreno-González**[1] | **Priscilla Rocío-Bautista**[1] | **David Parras-Guijarro**[3] | **Alberto Sánchez-Vizcaino**[3] | **Sebastian Brandt**[4] | **Juan F. García-Reyes**[1,2,3] | **Antonio Molina-Díaz**[1,2] | **Joachim Franzke**[4]

[1]Department of Physical and Analytical Chemistry, Analytical Chemistry Research Group, University of Jaén, Campus Las Lagunillas, Jaén, Spain

[2]University Research Institute for Olives Grove and Olive Oil, University of Jaén, Campus Las Lagunillas, Jaén, Spain

[3]University Research Institute for Iberian Archaeology, University of Jaén, Campus Las Lagunillas, Jaén, Spain

[4]ISAS—Leibniz Institut für Analytische Wissenschaften, Dortmund, Germany

Correspondence
Marcos Bouza, Analytical Chemistry Research Group, Department of Physical and Analytical Chemistry, University of Jaén, Campus Las Lagunillas, 23071 Jaén, Spain.
Email: mbouza@ujaen.es

Joachim Franzke, ISAS—Leibniz Institut für Analytische Wissenschaften, Dortmund, Germany.
Email: franzke@isas.de

Dielectric barrier discharge ionization has gained attention in the last few years due to its versatility and the vast array of molecules that can be ionized. In this study, we report on the assessment of liquid chromatography coupled to dielectric barrier discharge ionization with mass spectrometry for neutral lipid analysis. A set of different neutral lipid subclasses (triacylglycerides, diacylglycerides, and sterols) were selected for the study. The main species detected from our ionization source were $[M\text{-}H_2O+H]^+$, $[M+H]^+$ or $[M\text{-}R\text{-}H_2O+H]^+$, attributed to sterol dehydration, protonation or the fragmentation of an acyl chain accompanied by a water loss of the glycerolipids, respectively. In terms of sensitivity, the dielectric barrier discharge displayed overall improved abundances and comparable or better limits of quantitation than atmospheric pressure chemical ionization for both acylglycerols and sterols. As a case study, different archaeological samples with variable content in neutral lipids, particularly triacylglycerides, were studied. The identification was carried out by combining accurate mass and the tentative formula associated with the exact mass, retention time matching with standards, and additional structural information from in-source fragmentation. The high degree of unsaturation and the presence of sterols revealed the potential vegetal origin of the material stored in the analyzed samples.

KEYWORDS
dielectric barrier discharge, neutral lipids, liquid chromatography, mass spectrometry

Article Related Abbreviations: APCI, atmospheric pressure chemical ionization; Chol, cholesterol; DG, diacylglycerides; DBDI, dielectric barrier discharge ionization; EIC, extracted ion chromatogram; i-PrOH, isopropanol; MeOH, methanol; MG, monoacylglycerides; TG, triacylglycerides.

1 | INTRODUCTION

The constant evolution and technological improvements in MS have dramatically pushed the limits of lipid analysis [1, 2]. Lipid analysis, as well as any application in MS, necessitates an efficient manner to generate gas-phase ions. The appropriate ion source, solvent system and additives for lipid analysis are well studied and applied for different lipid categories (i.e. glycerophosphocholines, fatty acids), being ESI the chosen one for both shotgun [3] and LC lipidomics [4]. Glycerolipids and sterols analysis, among other neutral hydrophobic lipids, has been an analytical challenge despite their biological relevance [5, 6]. To characterize these species with ESI-MS, derivatization steps [7–9] and/or the use of modifiers promoting cationization (NH_4^+, Na^+, Li^+, etc.) [10–12] have been proposed, incurring the latter noticeable ion-suppression or matrix effects [13, 14].

Different ionization sources have been postulated as an alternative for MS analysis of nonpolar molecules, being atmospheric pressure chemical ionization (APCI) the more commonly studied [15–18]. The decoupling of desolvation and ionization during APCI reduces ion suppression and cationization competition. Plasma-based ion sources share standard features with APCI but also deliver unique characteristics that reaffirm them as an excellent alternative to consider for low polar molecules analysis [19]. Among these ionization methods, dielectric barrier discharge ionization (DBDI) has been gaining increasing attention because of its design versatility and easy construction [20], and outstanding performance for environmental analysis, food safety and imaging applications [21–25].

DBDs are generated between two electrodes with a dielectric barrier separating plasma and electrodes, ignited and sustained by AC voltage [26]. Still fruitfully researched in direct MS configurations, the use of DBDI for LC-MS analysis is yet under development and barely evaluated. Previous studies with DBDI using the housing from commercial APCI assemblies [27] have shown expanded chemical coverage, enhanced ionization efficiencies, and improved detection limits with respect to APCI and even ESI depending on the particular application [28–30]. Here, we report on the optimization and evaluation of a UHPLC DBDI-MS methodology for neutral lipid analysis. A set of different neutral lipid subclasses (triacylglycerides (TG), diacylglycerides (DG) and sterols) were selected for the study. A thorough optimization was carried out using cholesterol (Chol) and triolein (TG(18:1/18:1/18:1)) as representative species and paying particular attention to both the desolvation and the ion transmission steps. The sensitivity of the DBDI approach in terms of LOQ and S/N was evaluated. The method was successfully applied to the analysis of neutral lipids extracted from internal coverings of Roman storing archaeological structures made of mud and lime.

2 | MATERIALS AND METHODS

2.1 | Chemical and reagents

HPLC-grade methanol (MeOH) and isopropanol (i-PrOH) were purchased from Sigma-Aldrich (Madrid-Spain). A Milli-Q-Plus ultra-pure water system from Millipore (Milford, MA, USA) was used to obtain HPLC-grade water. Formic acid was purchased from Fluka (Buchs, Switzerland). The analytical-grade (> 99%) glycerolipid and sterol standards (see Table S1) were purchased from Sigma–Aldrich (Madrid, Spain).

2.2 | Optimization and calibration curves

Stock solutions of Chol (500 μg/ml) and TG(18:1/18:1/18:1) (100 μg/ml) were prepared in MeOH:i-PrOH (50:50). Three different replicates were performed to optimize the transmission voltage of the mass inlet capillary, spray drying gas flow, nebulizer pressure and drying gas temperature and vaporizer temperatures. The calibration solutions at different concentrations used for the linear calibration curves were prepared in MeOH:i-PrOH (50:50):

a. TG: mixtures of glyceryl trimyristate (TG(14:0/14:0/14:0)), glyceryl tripalmitate (TG(16:0/16:0/16:0)), glyceryl trilinoleate (TG(18:2/18:2/18:2)), glyceryl trilinolenate (TG(18:3/18:3/18:3)), glyceryl trioleate (TG(18:1/18:1/18:1)), glyceryl tristearate (TG(18:0/18:0/18:0)) with concentrations from 5 to 500 ng/ml.
b. DG: solutions of DL-α,β-distearin (DG(18:0/18:0)) with concentrations from 5 to 500 ng/ml.
c. Sterols: solutions of Chol, stigmasterol, and sitostanol with concentrations from 10 to 500 ng/ml.

2.3 | UHPLC coupled to TOF-MS

The chromatographic analyses were performed using a UHPLC Agilent 1290 Infinity (Agilent Technologies, Santa Clara, CA). It consists of a degasser, automatic sampler, a thermostated column compartment, and a binary pump. A Zorbax Rapid Resolution High Definition Eclipse-Plus C18 ($150 \times 4.6\ mm^2$, 1.8 μm particle size) (Agilent Technologies) UHPLC column was used. The chromatographic conditions were adjusted from a previous study [31]. During the chromatographic separation, the column temperature was

TABLE 1 Mass spectrometer optimized conditions for both ionization sources used in the present work

Parameter	DBDI	APCI
Vcap (V)	3000	3000
Vaporizer temperature (°C)	375	375
Drying gas temperature (°C)	325	350
Nebulizer pressure (psi)	40	60
Drying gas flow rate (L min^{-1})	3.3	5
Corona current (μA)	Non-applicable	4
Skimmer voltage (V)	65	65
Octapole rf (V)	250	250
Fragmentor voltage (V)	190	250

kept at 30°C, and 20 μl of sample/standards were injected in each run.

The UHPLC system was coupled to a time-of-flight mass spectrometer (Agilent 6220 accurate mass TOF (Agilent Technologies) for high-resolution MS measurements. The instrument is equipped with an APCI source. The DBDI probe was implemented to fit in the commercial source as described elsewhere [27, 32]. Figure S1 shows the scheme of the ionization source and a photo of the actual assembly. TOF analyses were performed in the positive ion mode, using different operating parameters for each ion source according to the results from the optimization study (Table 1).

A square-wave AC voltage with an amplitude of 3500 V was applied to the front electrode to generate the plasma of the DBDI probe, using an in-built high-voltage square waveform generator at a frequency of 20 kHz. Helium (purity 99.999%, Air Liquide, Spain) gas is used as discharge gas at a flow rate of 300 ml/min.

The MS instrument was daily calibrated using commercial Agilent low concentration APCI tuning mix solution (Agilent Technologies) using the APCI ion source. The full-scan data was recorded with Agilent MassHunter Data Acquisition software (version B.04.00) and processed with Agilent MassHunter Qualitative Analysis software (version B.04.00).

2.4 | Archaeological samples and sample treatment

The analyzed samples come from internal coverings of three archaeological structures for storage located in a Roman site (2nd–4th centuries AD) of Vilardida (Montferry and Vilarrodona, Tarragona, Spain). The structures have a rectangular trend shape (approximately 1 × 2 m and 50 cm deep). The coverings are made of mud and lime and serve to waterproof the interior wall. The samples were taken from the bottom of the structures and wrapped in dark paper, and stored in a freezer (at –20°C) until analysis. An appropriate amount (*ca*. 4 g) of the archaeological samples was collected. These sample portions were cleaned by removing the remained soil with an electric hand drill. After cleaning, the portions were grounded using a mortar and then, they were sieved in a mesh with 0.25 mm of opening.

The lipid extraction procedure for archaeological samples was adapted from the method described by Evershed et al. [12]. Each sample, previously ground, was treated as follows: a portion of 2 g was weighed in a glass centrifuge tube, where a 10-ml aliquot of $CHCl_3$:MeOH (2:1; v:v) was added. Then, the mixture was introduced into an ultrasonic bath for 15 min. Subsequently, the solution was centrifuged at 3500 rpm for 5 min, and the supernatant was separated and kept. The supernatant was evaporated until dryness under the N_2 stream. The dry extract was dissolved with 500 μl of $CHCl_3$ and stored until use at –20°C. To conduct UHPLC-MS measurements, 100 μl of the $CHCl_3$ extracted lipids were evaporated to dryness under the N_2 stream and reconstituted with 200 μl of i-PrOH, prior to UHPLC-MS measurements.

The data curation of the actual samples was done using MS-DIAL 4.60 for spectra deconvolution, peak detection, and MS-FINDER 3.50 for molecular formula prediction [33, 34]. The final compound annotation was done using the information obtained from MS-DIAL and MS-FINDER, and comparing the retention time information with available standards. The identification confidence level was designated following the criteria established by Schymanski et al. [35]. In the present case, most compounds can be described as tentative candidates matching a level three by using accurate mass measurements and the tentative formula associated with the exact mass, retention time matching with standards, and additional structural information from in-source fragmentation.

3 | RESULTS AND DISCUSSION

3.1 | LC coupled to DBDI-MS parameter optimization

Before any LC-MS analysis, a detailed optimization of the ionization source parameters was done. The used DBDI source requires the assessment of ion transmission parameters such as capillary voltage, drying gas pressure, inlet capillary temperature, and the evaluation of the vaporization-related parameters such as nebulizer pressure and vaporizer temperature. For optimization purposes, direct infusion of two representative model analytes was used: Chol and TG(18:1/18:1/18:1). The

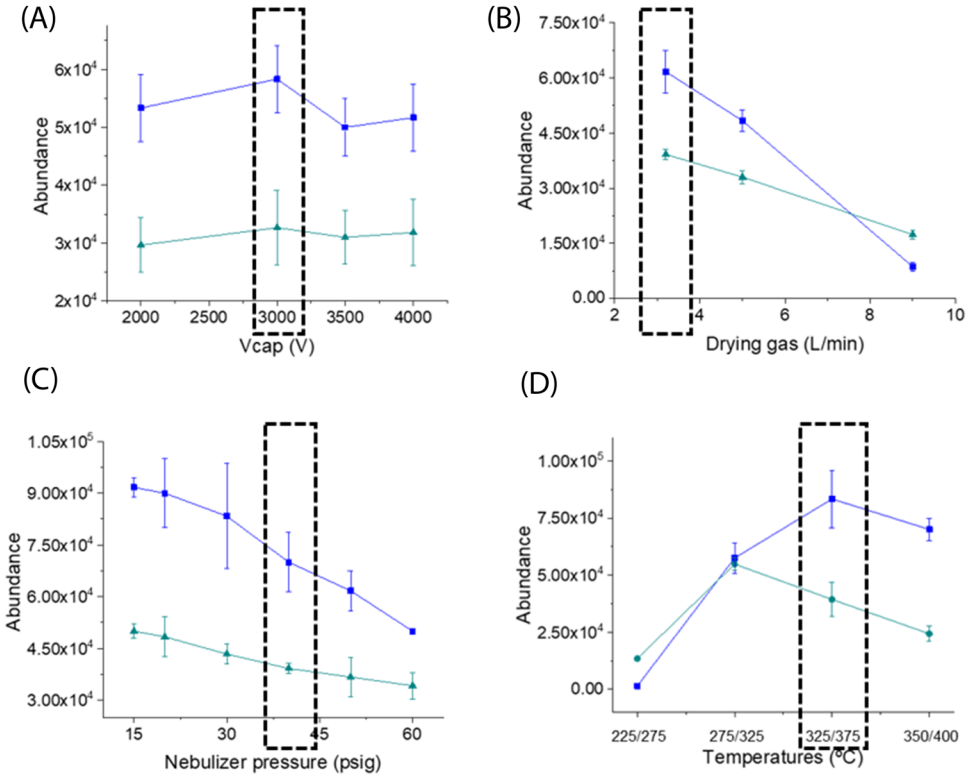

FIGURE 1 Abundances observed during the optimization of the vaporization and ion transmission parameters: (A) transmission voltage of the mass inlet capillary (Vcap), (B) drying gas flow, (C) vaporizer pressure, and (D) drying gas temperature and vaporizer temperatures. The Blue trace corresponds to the cholesterol signal as $[Chol\text{-}H_2O+H]^+$ with *m/z* 369.3482, and the green trace corresponds to the glyceryl triolate fragment signal as [DG(18:1/18:1)f -18:1-H2O+H]+ with *m/z* 603.5347. The optimum values selected are highlighted using a squared-dashed box

concentration used for the optimization was 500 ng/ml of Chol in MeOH:iPrOH (50:50, v:v) and 100 ng/ml of TG(18:1/18:1/18:1) in MeOH:iPrOH (50:50, v:v). The ion species used to evaluate the performance were: *m/z* 369 ($[M\text{-}H_2O+H]^+$) and *m/z* 603 ($[DG(18:1/18:1)_f\text{-}18:1\text{-}H_2O+H]^+$), respectively.

The reactant ions trajectories towards the mass inlet, and therefore the DBDI probe positioning, profoundly influence the abundances observed. The instrument spray chamber for APCI analysis presents two different probe inlets enabling two different orientations, defined as orthogonal (vaporizer and ion source at 90°) and axial (vaporizer and ion source at 45°). Both are operational, but the orthogonal one, being the same geometry as the APCI probe, proved the most efficient ionization (data not shown) for neutral lipids analysis. The angle of the probe with respect to the vaporizer flow on the orthogonal position was also critical; depicting the probe position as a clock, the probe should be oriented at 12, positioning the plasma towards the nebulized liquid stream (see Figure S1B). The capillary voltage was set at 3000 V, similarly to APCI, and, as observed in Figure 1A, this parameter has negligible influence on the observed signals. However, significant behavior differences were observed for the vaporizer and drying gas conditions. The TOF mass spectrometer utilizes a gas counterflow, named drying gas, to help with the nebulized droplets' desolvation and neutral removal prior to the MS inlet. A nitrogen stream is directed perpendicularly to the vaporizer towards the ion source. In the case of DBDI, the presence of high drying gas flows produced a drastic reduction of Chol and TG (18:1/18:1/18:1) abundances (Figure 1B). The different nitrogen flows, starting at 5 L/min, as opposed to the low helium discharge flow (0.300 L/min), hindered the ions transmission or disrupted reactions cascade for the reactant ions formation. DBDI operation required from lower drying gas flows, being selected as optimum 3.3 L/min (minimum instrumental operational value). Vaporizer nebulization pressure is also critical for the present ion source configuration. Although we observed higher abundances at lower pressure (Figure 1C), the background noise was also noteworthy. Note that, 40 psi was selected as optimum operational nebulizer pressure, striking a balance between absolute signal and appropriate S/N ratios. The greater abundances for all the observed ions (analytes and background ions) at lower vaporizer pressure are related to the

droplet size; lower pressures involve bigger droplet sizes and, hence, a higher number of species available for ionization but also promote a wider droplet size distribution. The gentleness of DBDI plasma enabled cleaner spectra with reduced background noise, compared to a corona discharge even when the operation nebulization pressure is lower (40 vs. 60 psi).

The temperatures required for the vaporization and droplet desolvation are crucial for sterol and TG analyses. Both are thermolabile compounds prone to dehydrate, in the case of sterols and fragments, in the case of TG, when energetic conditions are used. The optimization was done by pairing drying gas and vaporizing temperatures with a difference of 50°C, favoring higher temperatures in the vaporizer. As observed in Figure 1D, Chol and TG(18:1/18:1/18:1) exhibited two different trends. Chol showed an abundance boost when both temperatures were increased, reaching a plateau at the 350/400°C pair. Although higher temperatures promoted dehydration, they also favored a more efficient and homogeneous droplet desolvation.

On the other hand, TG(18:1/18:1/18:1) requires more precise temperature control. The higher abundances for $[DG(18:1/18:1)_f$ -18:1-$H_2O+H]^+$ were observed for 275/325°C, but the higher the temperature, the greater the abundances of the diglyceride and monoglyceride fragment ions detected for triolein. The final temperatures selected were 325/375°C as a compromise in terms of reproducibility and improved sensitivities while maintaining the presence of the intact TG protonated molecule. In general terms, most of the optimized introduction-ion transmission conditions selected for DBDI operation were milder than in APCI.

3.2 | Analytical performance of DBDI for neutral lipid analysis

The performance of the two ion sources was evaluated by using two separated mocking samples of glycerolipids and sterols with a concentration of 100 ng/ml of each component. For this evaluation, the LC-MS analyses were performed using the parameters above optimized and the APCI method previously reported as optimum [31]. As shown in Figure 2, the extracted ion chromatogram (EIC) for the most abundant *m/z* for each neutral lipid presented comparable and/or higher intensities when DBDI was used. The EIC for three different TG species: TG(18:3/18:3/18:3), TG(14:0/14:0/14:0) and TG(18:2/18:2/18:2), and monoacylglycerides (MG)(16:0) (Figure 2A–D) as well as for most of the glycerolipid standards evaluated, presented signals ~40% higher when analyzed with DBDI compared to APCI. The same trend was observed in the mass spectra (Figure S2). This enhancement agrees with previous reports where DBDI demonstrated lesser ion suppression and reduced matrix effects than APCI or ESI for pesticide and low polar contaminants analysis [27]. The ionization efficiency of the tested neutral lipids suggested greater populations of reactant ions, eventually leading to higher ionization yields for DBDI analysis.

The evaluated TG raised different fragments based on their thermal stability. Those compounds were likely to produce neutral losses when they were analyzed at the high vaporization temperatures or permit in-source fragmentations caused by the temperatures leading to a series of ion species such as TG protonated species, $[M+H]^+$, to the dehydration product ($[M\text{-}R\text{-}H_2O+H]^+$ or even the MG, $[M\text{-}2R\text{-}2H_2O+H]^+$.

Although APCI and plasma-based sources are often depicted as similar in behavior, we did observe differences. The dehydrated ion species, $[DG(18:0/18:0)\text{-}H_2O+H]^+$, of DL-α,β-distearin produced similar intensities for APCI and DBDI. However, as shown in Figure 2E inset, the areas of the EIC corresponding to *m/z* 341.31, at the retention time of the DG molecule, showed an increase of 54.2% in the analysis area detected when DBDI was used. The greater ionization efficiency observed for the DG(18:0/18:0) fragments enables better sensitivity for DBDI accompanied by a better knowledge of the tentative identification because of the inherent in-source fragmentation promoted by the ion source. The lack of tandem MS in our instrumentation was completed by the fragmentation promoted in the DBDI. The fragments and exact mass were harnessed later on to increase the species annotation reliance, something hard to tackle for ESI-MS analysis [36].

The signal increment was less noticeable regarding sterols, but DBDI offered peak areas 20% larger than APCI (see Figure 2F). The ionization of sterols is hardly achievable using ESI, referring to chemical and photoionization as alternatives [37, 38]. Dehydrated protonated sterol ions, $[M\text{-}H_2O+H]^+$ (i.e., Chol had an *m/z* 369.352) were observed, instead of the expected $[M+H]^+$ ions, when APCI and DBDI work as ion sources.

Different calibration curves were developed to evaluate the DBDI linearity and detection limits. The concentrations selected for TG and DG were in the range of 5–500 ng/ml. The lower abundances observed for sterols during the optimization and ion source comparison implied poorer ionization efficiency compared to glycerolipids. The sterols concentrations, for the linear calibrations, were in the range 10–1000 ng/ml for Chol and stigmasterol and between 50 and 1000 ng/ml for sitostanol. The EIC peak areas of the most abundant ion for each lipid within the ±25 mDa mass window was used to quantify. The S/N ratio corresponding to the lowest concentration detected

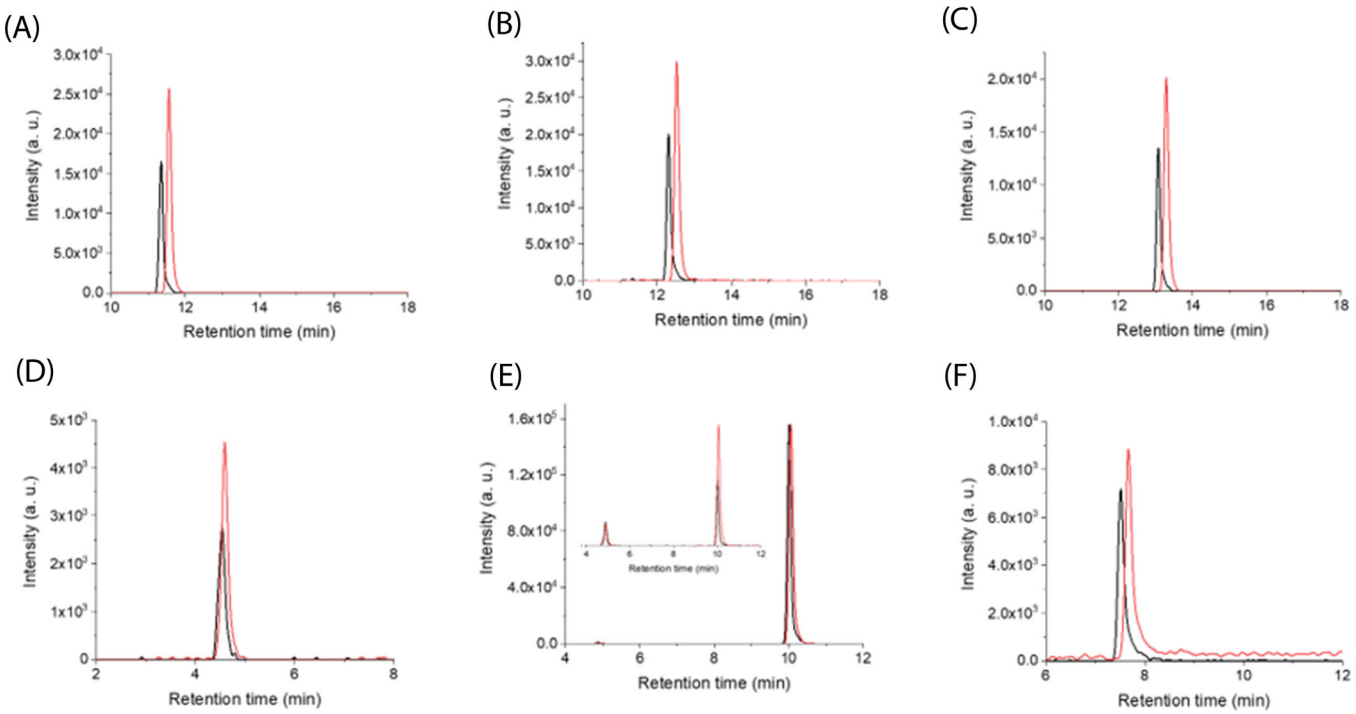

FIGURE 2 Extracted ion chromatogram (EIC) chromatograms for different glycerolipids and sterols (A) TG(18:3/18:3/18:3) ([TG(18:3/18:3/18:3)+H]$^+$ at *m/z* 873.70), (B) TG(14:0/14:0/14:0) (([DG(14:0/14:0)-14:0-H2O+H]$^+$ at *m/z* 495.44), (C) TG(18:2/18:2/18:2) ([TG(18:2/18:2/18:2)+H]$^+$ at *m/z* 879.74), (D) MG(16:0) ([MG(16:0)-H_2O+H]$^+$ at *m/z* 313.27), (E) DG(18:0/18:0) ([DG(18:0/18:0)-H_2O+H]$^+$ at *m/z* 607.57). The inset figure corresponded to [DG(16:0/16:0)-16:0)-H_2O+H]$^+$ at *m/z* 341.31 EIC. (F) Cholesterol ([Chol-H_2O+H]$^+$ at *m/z* 369.35). The black trace corresponds to APCI signals and the red trace to dielectric barrier discharge ionization (DBDI)

TABLE 2 Slopes, determination coefficient, the limit of quantification, and S/N of the minimum detected concentration for different glycerolipid and sterol standards using LC-DBDI-MS. In addition, LOQs and S/N for LC-APCI-MS analysis were included

Compound	Detected ion	DBDI Slope	*DBDI* R^2	DBDI LOQ (ng/ml)	APCI LOQ (ng/ml)	DBDI S/N	APCI S/N
DL-α,β-Distearin (DG(18:0/18:0))	[DG(18:0/18:0)-H_2O+H]$^+$	14 651	0.9997	0.4	0.4	125.7	135.7
DL-α,β-Distearin (DG(18:0/18:0))	[MG(18:0)$_f$-H_2O+H]$^+$	7040.2	0.9997	1.6	3.2	30.6	15.7
Glyceryl trimyristate (TG(14:0/14:0/14:0))	[DG(14:0/14:0)$_f$-H_2O+H]$^+$	2460.9	0.9997	1.6	3.4	31.0	14.7
Glyceryl tripalmitate (TG(16:0/16:0/16:0))	[DG(16:0/16:0)$_f$-H_2O+H]$^+$	2223.6	0.9996	4.0	5.5	12.4	9.1
Glyceryl trilinoleate (TG(18:2/18:2/18:2))	[TG(18:2/18:2/18:2)+H]$^+$	1590.9	0.9992	2.4	5.2	20.5	9.6
Glyceryl trioleate (TG(18:1/18:1/18:1))	[DG(18:1/18:1)$_f$-H_2O+H]$^+$	3318.5	0.9993	3.2	3.6	15.7	13.7
Glyceryl tristearate (TG(18:0/18:0/18:0))	[DG(18:0/18:0)H_2O+H]$^+$	2298.6	0.9996	5.2	5.6	9.7	8.9
Glyceryl trilinolenate (TG(18:3/18:3/18:3))	[TG(18:3/18:3/18:3)+H]$^+$	2403.5	0.9999	1.1	1.1	46.5	46.0
Cholesterol (Chol)	[Chol-H_2O+H]$^+$	1130.5	0.999	14.3	19.6	7.0	5.1
Stigmasterol (Stig)	[Stig-H_2O+H]$^+$	463.41	0.9993	24.4	28.6	4.1	3.5
Sitostanol (Sitos)	[Sitos-H_2O+H]$^+$	89.444	0.9954	64.9	62.5	7.7	8.0

was used to calculate the LOQ. The slope, coefficient of determination and LOQ are collected in Table 2.

To evaluate the optimized LC-DBDI-MS method's further applicability for neutral lipids and its reproducibility, ten independent replicates of a mixture containing eight different compounds, representative of the studied lipid subclasses, were done. The robustness of the method was demonstrated by the little variation in retention times between replicates (Figure S3) and the minimum RSD observed for the detected abundances (Table S2).

3.3 | Lipid profiling of archaeological samples

The DBDI neutral lipid analysis applicability was evaluated by using lipid extracts from storing structures coverings. The lipid content of archaeological materials (ceramic, storing structures, wall paintings, etc.) is a relevant and timely topic in archaeometry, helping to understand ancient societies' working processes, rituals, and dietary habits [39, 40]. Three archaeological samples were analyzed using LC-DBDI-MS. High-resolution MS measurements and retention time was used to correlate the measured *m/z* with glycerolipids and sterols identified species in archaeological samples (mainly ceramics) previously analyzed in other similar studies [31]. MS-DIAL 4.60 and MS-FINDER were used to curate the data and help with the identification of the detected ions.

The level of certainty in our identification is restricted to accurate mass measurements and the tentative formula associated with the detected *m/z*, the retention time comparison with standards, and additional information from in-source fragmentation readily available with the full-scan acquisition. In the case of unknown species, not previously assigned or standard matched, the identification was made by comparing the retention time similarity with the standards, the number of carbons assigned by tentative formula matching, and DG fragments observed at the same retention times of TG intact ion. Table 3 and Table S3 and S4 collect the manually curated data. Most of the species identified agreed with species detected previously, although we did not use a reference technique, such as GC-MS, to corroborate the identification.

The compounds identified in three evaluated samples (S1, S2, and S3) presented a high degree of unsaturation and high intensities for sterols, likely attributed to vegetable oil storage in the structures. Although possible, the absence of tandem MS information hampered the annotation of the fatty acyl chain compositions for the detected TG.

Despite reporting a few dozens of compounds for each sample, we are aware that the lipid composition of these samples is far more complex in number and species type. Oxidation, degradation, and hydrolysis of the molecules should be present, but those are not the target of the present study. Further studies, like a detailed analysis of the composition and the significance of the potential compounds present in the samples evaluated in this work, will be elaborated to help with the interpretation and gain profound knowledge of the sample origin. Besides that, we will aggregate tandem MS to facilitate isomer depiction among the different compounds identified.

4 | CONCLUDING REMARKS

We have reported the first application of DBDI for neutral lipid analysis including TG and sterols using archaeological samples as a case study. We proposed DBDI as an alternative ion source for the analysis of those compounds, with precision and sensitivity at the level, or outperforming commercial instrumentation. Although seemingly related to the ion source, the different drying gas and vaporizer temperatures played a critical role in the glycerolipid structural integrity enabling more informative spectra, with protonated and fragment ions detected at once, for MS (without tandem MS). The calibration curves for APCI and DBDI analysis showed boosted sensitivities, in most of the evaluated cases, favoring the AC operated ion source. The potential of DBDI was assessed by analyzing real samples, in this case, using actual samples of archaeological origin. This work laid the foundations for further research in lipidomics using DBDI related ion sources. Future research seems mandatory to evaluate the behavior of this method for complex samples, in terms of lipid content and polarity range.

ACKNOWLEDGMENTS

This work was supported by the Spanish Ministerio de Economía y Competitividad (MINECO) through Project Ref. PID2019-107691RB-I00. The financial support from the Ministerium für Innovation, Wissenschaft und Forschung des Landes Nordrhein-Westfalen, the Senatsverwaltung für Wirtschaft, Technologie und Forschung des Landes Berlin, the Ministerium für Bildung und Forschung and the Deutsche Forschungsgemeinschaft is gratefully acknowledged. B.G.L. also thanks the Spanish Ministerio de Ciencia e Innovación for her Ramón y Cajal postdoctoral research contract (ref. RYC2019-026581-I). The authors acknowledge the assistance of Rocio Nortes, Felipe J. Lara-Ortega, and José Robles-Molina for their support during preliminary studies of DBDI method development, and also they acknowledge Dr. Xavier Clop from the Autonomous University of Barcelona for providing the archeological samples.

TABLE 3 Glycerolipids and sterols ions detected and identified for LC-DBDI-MS analysis for sample S1. The sub-index f corresponded to a diacylglyceride (DG) as a potential fragment of a triacylglyceride (TG); precursors and potential fragments are correlated in the table if the retention time matches and, if that is the case, the compounds are shadowed in the same color. Abbreviations: Sito = sitostanol, 18:2 = linoleic acid, 18:1 = oleic acid, 16:1 = palmitoleic acid, 16:0 = palmatic acid, 18:0 = stearic acid

Retention time (min)	2017 identification[26]	Compound	*m/z* exp	Precursor type	Tentative formula	Mass error (mDa)
7.98	$[Sitos\text{-}H_2O+H]^+$	Sitosterol	397.3835	$[M\text{-}H_2O+H]^+$	$C_{29}H_{48}$	-0.65
11.30		$DG(34:3)_f$	573.4842	$[M\text{-}H_2O+H]^+$	$C_{37}H_{64}O_4$	3.51
11.41	$[DG(18:2/18:2)_f\text{-}H_2O+H]^+$	$DG\ (36:4)_f$	599.5016	$[M\text{-}H_2O+H]^+$	$C_{39}H_{66}O_4$	1.76
11.77		TG (52:7)	849.6923	[M+H]+	$C_{55}H_{92}O_6$	4.34
12.01		$DG(34:4)_f$	571.4751	$[M\text{-}H_2O+H]^+$	$C_{37}H_{62}O_4$	-3.06
12.01	$[DG(18:1/18:2)_f\text{-}H_2O+H]^+$	$DG\ (36:3)_f$	601.5173	$[M\text{-}H_2O+H]^+$	$C_{39}H_{68}O_4$	1.71
12.01		TG (50:6)	825.6951	[M+H]+	$C_{53}H_{92}O_6$	1.54
12.30		$DG\ (30:1)_f$	521.4554	$[M\text{-}H_2O+H]^+$	$C_{33}H_{60}O_4$	1.01
12.33		TG (46:2)	775.6798	$[M+H]^+$	$C_{49}H_{90}O_6$	1.19
12.39	$[DG(16:1/16:1)_f\text{-}H_2O+H]^+$	$DG\ (32:2)_f$	547.4709	$[M\text{-}H_2O+H]^+$	$C_{35}H_{62}O_4$	1.16
12.40	$[TG(16:1/16:/16:1)+H]^+$	TG (48:3)	801.6952	$[M+H]^+$	$C_{51}H_{92}O_6$	1.44
12.59		$DG(34:3)_f$	573.4853	$[M\text{-}H_2O+H]^+$	$C_{37}H_{64}O_4$	2.41
12.59		TG (52:6)	851.7098	$[M+H]^+$	$C_{55}H_{94}O_6$	2.49
12.63	$[DG(18:1/18:1)_f\text{-}H_2O+H]^+$	$DG\ (36:2)_f$	603.5330	$[M\text{-}H_2O+H]^+$	$C_{39}H_{70}O_4$	1.66
12.77		TG (50:5)	827.7085	$[M+H]^+$	$C_{53}H_{94}O_6$	3.79
12.91		$DG(34:4)_f$	571.4704	$[M\text{-}H_2O+H]^+$	$C_{37}H_{62}O_4$	1.66
12.95		TG (52:5)	853.7250	$[M+H]^+$	$C_{55}H_{96}O_6$	2.94
13.02		$DG\ (30:1)_f$	521.4558	$[M\text{-}H_2O+H]^+$	$C_{33}H_{60}O_4$	0.61
13.02		TG (46:1)	777.6947	$[M+H]^+$	$C_{49}H_{92}O_6$	1.94
13.02	$[TG(18:2/18:2/18:2)+H]^+$	TG (54:6)	879.7418	$[M+H]^+$	$C_{57}H_{98}O_6$	1.79
13.08	$[DG(16:1+16:0)_f\text{-}H_2O+H]^+$	$DG(32:1)_f$	549.4861	$[M\text{-}H_2O+H]^+$	$C_{35}H_{64}O_4$	1.61
13.08	[TG(16:1+16:0+16:1)+H]	TG (48:2)	803.7098	$[M+H]^+$	$C_{51}H_{94}O_6$	2.49
13.10	$[DG(16:1/16:1)_f\text{-}H_2O+H]^+$	$DG(32:2)_f$	547.4706	$[M\text{-}H_2O+H]^+$	$C_{35}H_{62}O_4$	1.46
13.20	$[DG(16:0+18:2)_f\text{-}H_2O+H]^+$	$DG\ (34:2)_f$	575.5023	$[M\text{-}H_2O+H]^+$	$C_{37}H_{66}O_4$	1.06
13.21		TG (50:4)	829.7228	$[M+H]^+$	$C_{53}H_{96}O_6$	5.14
13.49	$[TG(18:2/16:0/18:2)+H]^+$	TG (52:4)	855.7366	$[M+H]^+$	$C_{55}H_{98}O_6$	6.99
13.54	$[DG(18:2/18:2)_f\text{-}H_2O+H]^+$	$DG\ (36:4)_f$	599.5027	$[M\text{-}H_2O+H]^+$	$C_{39}H_{66}O_4$	0.66
13.54	$[DG(18:1+18:2)_f\text{-}H_2O+H]^+$	$DG\ (36:3)_f$	601.5178	$[M\text{-}H_2O+H]^+$	$C_{39}H_{68}O_4$	1.21
13.57	$[DG(18:2/18:1/18:2)+H]^+$	TG (54:5)	881.7549	[M+H]+	$C_{57}H_{100}O_6$	4.34
13.85	$[DG(16:0+18:2)_f\text{-}H_2O+H]^+$	$DG\ (34:2)_f$	575.5023	$[M\text{-}H_2O+H]^+$	$C_{37}H_{66}O_4$	1.06
13.85		TG (50:3)	831.7382	[M+H]+	$C_{53}H_{98}O_6$	5.39
14.02	$[DG(16:0+18:2)_f\text{-}H_2O+H]^+$	$DG\ (34:2)_f$	575.5023	$[M\text{-}H_2O+H]^+$	$C_{37}H_{66}O_4$	1.06
14.03	$[TG(16:0/18:2/18:1)+H]^+$	TG (52:3)	857.7592	$[M+H]^+$	$C_{55}H_{100}O_6$	0.04

(Continues)

TABLE 3 (Continued)

Retention time (min)	2017 identification[26]	Compound	*m/z* exp	Precursor type	Tentative formula	Mass error (mDa)
14.19	[DG(18:1+18:2)$_f$ -H_2O+H]$^+$	DG (36:3)	601.5181	[M-H_2O+H]$^+$	$C_{39}H_{68}O_4$	0.91
14.19	[TG(18:1/18:2/18:1)+H]$^+$	TG (54:4)	883.7738	[M+H]$^+$	$C_{57}H_{102}O_6$	1.09
14.58	[DG(16:0+18:1)$_f$ -H_2O+H]$^+$	DG (34:1)$_f$	577.5144	[M-H_2O+H]$^+$	$C_{37}H_{68}O_4$	4.61
14.6	[TG(18:1/16:0/18:1)+H]$^+$	TG (52:2)	859.7720	[M+H]$^+$	$C_{55}H_{102}O_6$	2.89
14.67	[DG(18:1/18:1)$_f$ -H_2O+H]$^+$	DG (36:2)$_f$	603.5330	[M-H_2O+H]$^+$	$C_{39}H_{70}O_4$	1.66
14.68	[TG(18:1/18:1/18:1)+H]$^+$	TG (54:3)	885.7880	[M+H]$^+$	$C_{57}H_{104}O_6$	2.54
15.34	[DG(18:1+18:0)$_f$ -H_2O+H]$^+$	DG (36:1)$_f$	605.5478	[M-H_2O+H]$^+$	$C_{39}H_{72}O_4$	2.51
15.40		DG (38:2)$_f$	631.5631	[M-H_2O+H]$^+$	$C_{41}H_{74}O_4$	2.86

CONFLICT OF INTEREST

The authors declare no conflict of interest.

DATA AVAILABILITY STATEMENT

The data generated in this work are available from the correponding authors on reasonable request.

ORCID

Marcos Bouza https://orcid.org/0000-0002-2601-9776

REFERENCES

1. Rustam YH, Reid GE. Analytical challenges and recent advances in mass spectrometry based lipidomics. Anal Chem. 2018;90:374–97.
2. Hu T, Zhang J-L. Mass-spectrometry-based lipidomics. J Sep Sci. 2018;41:351–72.
3. Wang M, Wang C, Han RH, Han X. Novel advances in shotgun lipidomics for biology and medicine. Prog Lipid Res. 2016;61:83–108.
4. Ivanova PT, Milne SB, Myers DS, Brown HA. Lipidomics: a mass spectrometry based systems level analysis of cellular lipids. Curr Opin Chem Biol. 2009;13:526–531.
5. Murphy RC, Leiker TJ, Barkley RM. Glycerolipid and cholesterol ester analyses in biological samples by mass spectrometry. Biochimica et Biophysica Acta (BBA) - Mol Cell Biol Lipids. 2011;1811:776–783.
6. Gachumi G, El-Aneed A. Mass spectrometric approaches for the analysis of phytosterols in biological samples. J Agric Food Chem. 2017;65:10141–10156.
7. Leiker TJ, Barkley RM, Murphy RC. Analysis of diacylglycerol molecular species in cellular lipid extracts by normal-phase LC-electrospray mass spectrometry. Int J Mass spectrom. 2011;305:103–108.
8. Yang FQ, Feng K, Zhao J, Li SP. Analysis of sterols and fatty acids in natural and cultured Cordyceps by one-step derivatization followed with gas chromatography–mass spectrometry. J Pharm Biomed Anal. 2009;49:1172–1178.
9. Avula SGC, Belovich JM, Xu Y. Determination of fatty acid methyl esters derived from algae Scenedesmus dimorphus biomass by GC–MS with one-step esterification of free fatty acids and transesterification of glycerolipids. J Sep Sci. 2017;40:2214–2227.
10. Hsu F-F, Turk J. Electrospray ionization multiple-stage linear ion-trap mass spectrometry for structural elucidation of triacylglycerols: Assignment of fatty acyl groups on the glycerol backbone and location of double bonds. J Am Soc Mass Spectrom. 2010;21:657–669.
11. Herrera LC, Potvin MA, Melanson JE. Quantitative analysis of positional isomers of triacylglycerols via electrospray ionization tandem mass spectrometry of sodiated adducts. Rapid Commun Mass Spectrom. 2010;24:2745–2752.
12. Samburova V, Lemos MS, Hiibel S, Kent Hoekman S, Cushman JC, Zielinska B. Analysis of triacylglycerols and free fatty acids in algae using ultra-performance liquid chromatography mass spectrometry. J Am Oil Chem Soc. 2013;90:53–64.
13. Mallet CR, Lu Z, Mazzeo JR. A study of ion suppression effects in electrospray ionization from mobile phase additives and solid-phase extracts. Rapid Commun Mass Spectrom. 2004;18:49–58.
14. Taylor PJ. Matrix effects: the Achilles heel of quantitative high-performance liquid chromatography–electrospray–tandem mass spectrometry. Clin Biochem. 2005;38:328–334.
15. Byrdwell WC, Neff WE. Dual parallel electrospray ionization and atmospheric pressure chemical ionization mass spectrometry (MS), MS/MS and MS/MS/MS for the analysis of triacylglycerols and triacylglycerol oxidation products. Rapid Commun Mass Spectrom. 2002;16:300–319.
16. Holčapek M, Lísa M, Jandera P, Kabátová N. Quantitation of triacylglycerols in plant oils using HPLC with APCI-MS, evaporative light-scattering, and UV detection. J Sep Sci. 2005;28:1315–1333.
17. Fasciotti M, Pereira Netto AD. Optimization and application of methods of triacylglycerol evaluation for characterization of olive oil adulteration by soybean oil with HPLC–APCI-MS–MS. Talanta 2010;81:1116–1125.
18. Fanali C, Beccaria M, Salivo S, Tranchida P, Tripodo G, Farnetti S, Dugo L, Dugo P, Mondello L. Non-polar lipids characterization of Quinoa (Chenopodium quinoa) seed by comprehensive two-dimensional gas chromatography with flame ionization/mass spectrometry detection and non-aqueous reversed-phase liquid chromatography with atmospheric

pressure chemical ionization mass spectrometry detection. J Sep Sci. 2015;38:3151–3160.
19. Ding X, Duan Y. Plasma-based ambient mass spectrometry techniques: the current status and future prospective. Mass Spectrom Rev. 2015;34:449–473.
20. Meyer C, Müller S, Gurevich EL, Franzke J. Dielectric barrier discharges in analytical chemistry. Analyst. 2011;136:2427–2440.
21. Zhang H, Jiang J, Li N, Li M, Wang Y, He J, You H. Surface desorption dielectric-barrier discharge ionization mass spectrometry. Anal Chem. 2017;89:7333–7339.
22. Elia EA, Niehaus M, Steven RT, Wolf J-C, Bunch J. Atmospheric pressure MALDI mass spectrometry imaging using in-line plasma induced postionization. Anal Chem. 2020;92:15285–15290.
23. Gyr L, Wolf J-C, Franzke J, Zenobi R. Mechanistic understanding leads to increased ionization efficiency and selectivity in dielectric barrier discharge ionization mass spectrometry: a case study with perfluorinated compounds. Anal Chem. 2018;90:2725–2731.
24. Weber M, Wolf J-C, Haisch C. Gas chromatography–atmospheric pressure inlet–mass spectrometer utilizing plasma-based soft ionization for the analysis of saturated, aliphatic hydrocarbons. J Am Soc Mass Spectrom. 2021;32:1707–1715.
25. Lu Q, Guan X, You X, Xu Z, Zenobi R. High-spatial resolution atmospheric pressure mass spectrometry imaging using fiber probe laser ablation-dielectric barrier discharge ionization. Anal Chem. 2021;93:14694–14700.
26. Niu G, Knodel A, Burhenn S, Brandt S, Franzke J. Review: Miniature dielectric barrier discharge (DBD) in analytical atomic spectrometry. Anal Chim Acta. 2020.
27. Lara-Ortega FJ, Robles-Molina J, Brandt S, Schütz A, Gilbert-López B, Molina-Díaz A, García-Reyes JF, Franzke J. Use of dielectric barrier discharge ionization to minimize matrix effects and expand coverage in pesticide residue analysis by liquid chromatography-mass spectrometry. Anal Chim Acta. 2018;1020:76–85.
28. Gilbert-López B, Lara-Ortega FJ, Robles-Molina J, Brandt S, Schütz A, Moreno-González D, García-Reyes JF, Molina-Díaz A, Franzke J. Detection of multiclass explosives and related compounds in soil and water by liquid chromatography-dielectric barrier discharge ionization-mass spectrometry. Anal BioanalChem. 2019;411:4785–4796.
29. Schütz A, Brandt S, Liedtke S, Foest D, Marggraf U, Franzke J. Dielectric barrier discharge ionization of perfluorinated compounds. Anal Chem. 2015;87:11415–11419.
30. Mirabelli MF, Wolf J-C, Zenobi R. Pesticide analysis at ppt concentration levels: coupling nano-liquid chromatography with dielectric barrier discharge ionization-mass spectrometry. Anal BioanalChem. 2016;408:3425–3434.
31. Tuñón-López JA, Beneito-Cambra M, Robles-Molina J, Parras-Guijarro DJ, Molina-Díaz A, Sánchez-Vizcaíno A, García-Reyes JF. Multiclass profiling of lipids of archaeological interest by ultra-high pressure liquid chromatography-atmospheric pressure chemical ionization-high resolution mass spectrometry. Microchem J. 2017;132:49–58.
32. Schütz A, Lara-Ortega FJ, Klute FD, Brandt S, Schilling M, Michels A, Veza D, Horvatic V, García-Reyes JF, Franzke J. Soft argon–propane dielectric barrier discharge ionization. Anal Chem. 2018;90:3537–3542.
33. Tsugawa H, Ikeda K, Takahashi M, Satoh A, Mori Y, Uchino H, Okahashi N, Yamada Y, Tada I, Bonini P, Higashi Y, Okazaki Y, Zhou Z, Zhu Z-J, Koelmel J, Cajka T, Fiehn O, Saito K, Arita M, Arita M. A lipidome atlas in MS-DIAL 4. Nat Biotechnol. 2020;38:1159–1163.
34. Lai Z, Tsugawa H, Wohlgemuth G, Mehta S, Mueller M, Zheng Y, Ogiwara A, Meissen J, Showalter M, Takeuchi K, Kind T, Beal P, Arita M, Fiehn O. Identifying metabolites by integrating metabolome databases with mass spectrometry cheminformatics. Nat Methods. 2018;15:53–56.
35. Schymanski EL, Jeon J, Gulde R, Fenner K, Ruff M, Singer HP, Hollender J. Identifying Small Molecules via High Resolution Mass Spectrometry: Communicating Confidence. Environ Sci Technol. 2014;48:2097–2098.
36. Beccaria M, Inferrera V, Rigano F, Gorynski K, Purcaro G, Pawliszyn J, Dugo P, Mondello L. Highly informative multiclass profiling of lipids by ultra-high performance liquid chromatography – Low resolution (quadrupole) mass spectrometry by using electrospray ionization and atmospheric pressure chemical ionization interfaces. J Chromatogr A. 2017;1509:69–82.
37. Palmgrén JJ, Töyräs A, Mauriala T, Mönkkönen J, Auriola S. Quantitative determination of cholesterol, sitosterol, and sitostanol in cultured Caco-2 cells by liquid chromatography–atmospheric pressure chemical ionization mass spectrometry. J Chromatogr B. 2005;821:144–152.
38. Grün CH, Besseau S. Normal-phase liquid chromatography–atmospheric-pressure photoionization–mass spectrometry analysis of cholesterol and phytosterol oxidation products. J Chromatogr A. 2016;1439:74–81.
39. Giorgi G. Overview of mass spectrometric based techniques applied in the cultural heritage field. Organic Mass Spectrometry in Art and Archaeology. West Sussex: John Wiley & Sons; 2009. pp.7#x000A0;37–74.
40. Colombini MP, Modugno F. Organic materials in art and archaeology. Organic Mass Spectrometry in Art and Archaeology. West Sussex: John Wiley & Sons; 2009. pp. 1–36.

SUPPORTING INFORMATION

Additional supporting information can be found online in the Supporting Information section at the end of this article.

How to cite this article: Bouza M, García-Martínez J, Gilbert-López B, Moreno-González D, Rocío-Bautista P, Parras-Guijarro D, et al. Liquid chromatography-dielectric barrier discharge ionization mass spectrometry for the analysis of neutral lipids of archaeological interest. J Sep Sci. 2022;45:3105–3114.
https://doi.org/10.1002/jssc.202200402